Journal of Innovative Technology, Vol. 1, No. 2, pp. 41-46 September 2019
http://doi.org/10.29424/JIT.201909_1(2).0007


# GEOMETRIC STRUCTURE ENHANCED NITROGEN GAS SENSING ABILITY FROM CARBON NANOTUBES

Yung-Huang Chang [1*], Yuan-Tsung Chen [2], and Chien-Sheng Huang [3]

## ABSTRACT

For decades, the nanostructure of carbon nanotubes (CNTs) have attracted ample attention in the application of gas sensors. However, those CNT-based gas sensors are mostly manufactured in the single or film structures. Until now, the CNT bundle structure in gas sensors has not yet been investigated by researchers. In this study, the effects of the film and the bundle structure in CNTs are explored. The abundant interstitial and groove sites, beneficial for $N_2$ gas absorption and charge transfer, were provided through the CNT bundle with particular geometric structures. In terms of detecting nitrogen gas, the CNT bundle is found to have significantly superior sensitivity, faster response and recover time, comparing to the CNT film. Therefore, the geometric structure of CNTs is approved to be one of the features the designers of the gas sensor should take into consideration in the future.

*Keywords:* Gas sensor; CNT film; CNT bundle; thermal CVD.

## 1. INTRODUCTION

Due to the unique physical and chemical characteristics of the nanostructural materials, such as carbon nanotubes (CNTs) (Ong *et al*. 2002; Wong *et al*. 2003; Chopra *et al*. 2002; Modi *et al*. 2003; Chopra *et al*. 2003; Varghese *et al*. 2001), anodized nanostructures (Lee and Park 2014; Chang *et al*. 2012; Chang *et al*. 2018), graphene (Novoselov *et al*. 2004) and 2D transition metal dichalcogenides (Chang *et al*. 2014; Chang *et al*. 2014; Chang *et al*. 2014; Chang *et al*. 2013), nanotechnology has attracted a lot of attention for decades. Among them, CNTs possessing excellent conductivity (Futaba *et al*. 2006), one-dimensional nanostructures (Xia *et al*. 2003), high specific surface area and superior surface-area-to-volume ratio render themselves have the potential in the gas sensing applications. Gas sensors can be used for the purposes of environmental monitoring. When toxic gases are leaking, gas sensors can detect the leaking and prevent the potential damage to humans. Traditional gas sensors usually use semiconductor oxides as materials since they are safe, sensitive, and inexpensive. However, the chemical reaction between the materials and the target gas molecules can only be activated in the high temperature. (Tang *et al*. 1995) This condition has inhibited the development and the applications of traditional gas sensors. Researchers have found that the CVD-grown CNTs are capable to function in the room temperature. (Qi *et al*. 2003) They have become one of the most promising materials to manufacture gas sensors. Gas sensors will usually operate in two mechanisms: gas adsorption (Korotcenkov 2007; Huang *et al*. 2005) and gas ionization. (Modi *et al*. 2003; Lin *et al*. 2012) Gas adsorption is a common detection method based on the change of electrical properties. (Cantalini *et al*. 2003; Liang *et al*. 2004; Jang *et al*. 2004; Li *et al*. 2003) Due to the differences in charge transfer, the detected gas can be classified into reducing and oxidizing gaseous species. (Tomchenko *et al*. 2003) For example, if being exposed to reducing gaseous species, such as $NH_3$ (Chopra *et al*. 2003), $CO_2$ (Ong *et al*. 2002; Varghese *et al*. 2001), $N_2$ (Zhao *et al*. 2002) and ethanol (Pàez *et al*. 2004) etc., the electrical resistance of p-type CNTs will be found to increase, indicating the electron transfer from the gases to CNTs. On the contrary, if being exposed to oxidizing gaseous species, such as $O_2$ (Collins *et al*. 2000) and $NO_2$ (Kong *et al*. 2000), the electrical resistance of p-type CNTs will be found to decrease, indicating a different electron transfer from the gases to CNTs. In this study, $N_2$ absorption mechanism is investigated using the gas sensors of CNT film and CNT bundle. Because of the interstitial and groove sites in the CNT bundle, the $N_2$ absorption activity and the amount of charge transfer will be increased. The geometric structure of CNTs is proved to be the factor influencing the detection of $N_2$ gas.

## 2. MATERIALS AND METHODS

The vertically aligned carbon nanotubes were grown by using thermal chemical vapor deposition (CVD). The detail growing method was mentioned in the previous research. (Huang *et al*. 2005) The growing process was summarized in the following: First, a 30 nm Fe layer serving as a catalyst was deposited on n-type (100) Si substrates, using RF sputtering and Ar plasma. Before the growth of CNT, the Fe/Si substrates were pretreated in a CVD quartz tube under 6.5 Torr at 600 °C for 20 min, where high purity $N_2$ gas (99.999%) was used as carrier gas with a 100 sccm flow rate. Subsequently, for the synthesis of CNTs, the quartz tube was heated up to the 700 °C for 10 min under 3.5 Torr with a 30 sccm

Manuscript received January 31, 2019; revised June 16, 2019; accepted July 16, 2019.
[1*] Project Assistant Professor (corresponding author), Bachelor Program in Interdisciplinary Studies, National Yunlin University of Science and Technology, Yunlin, Taiwan, 64002, R.O.C. (e-mail: changyhu@yuntech.edu.tw).
[2] Distinguished Professor, Graduate School of Materials Science, National Yunlin University of Science and Technology, Yunlin, Taiwan, 64002, R.O.C.
[3] Assistant Professor, Department of Electronic Engineering, National Yunlin University of Science and Technology, Yunlin, Taiwan, 64002, R.O.C.

$C_2H_2$ gas flow rate. After the growth of CNTs, the quartz tube was then naturally cooled down to the room temperature in $N_2$. The CNT bundles were fabricated via tweezers, which were charged through friction with two contact surfaces.

The $N_2$ gas detection experiment was carried out by using an ultrahigh vacuum measurement system. In order to complete an outgassing process, the samples were biased at 1 voltage in an ultrahigh vacuum environment of $10^{-7}$ Torr for 1 hour prior to each measurement. The $N_2$ gas was detected via the changes of CNT resistance in an on/off $N_2$ environment at various bias voltages from 1V to 10V. Then the $N_2$ concentration was changed from 0.05 Torr to 500 Torr. All experiments were accomplished in the room temperature. The two electrodes, source and drain, were fabricated on the top of CNT film via the screen printing technology, using silver paster as the contact material. The current characteristics of all the samples were recorded using a Keithley 237 source-meter. Surface morphology of the CNT nanostructures was examined by a field-emission scanning electron microscope (FESEM, JSM-6500F) and a transmission electron microscope (TEM, JEM-2100F). Raman spectra were used to identify the composition of the samples, and the exciting laser wavelength was found to be 532 nm. Si peak at 520 cm−1 was used as a reference for calibration in Raman characterization.

## 3. RESULTS AND DISCUSSION

Surface morphology of the CNT film and bundle was displayed in Fig. 1. The typical cross-sectional and top-view SEM images of the vertically aligned CNT film were shown in Figs. 1 (a) and (b), respectively. The length was ~10 μm and the diameter was ~ 32 nm. Besides, the vapor-liquid-solid (VLS) growth mechanism was confirmed through the observation of Fe catalyst on the top of the CNTs, as shown in Fig. 1 (c). (Wagner 1964) The top-view SEM images of the CNT bundle were exhibited in different magnification in Figs. 1 (d) to (f). The length and diameter of the CNT bundle were 1.65 mm and 40 μm, respectively. Compared with CNT film, the CNT bundle was found to be more ordered and intensive in arrangement, which was useful in $N_2$ gas detection.

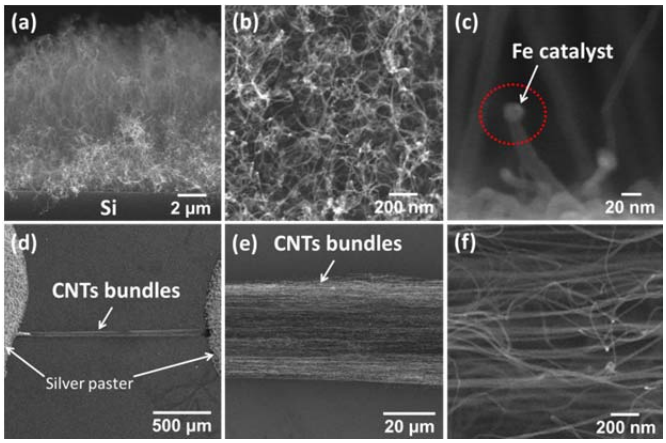


**Fig. 1 The typical (a) cross-sectional and (b) top-view SEM images of the vertical aligned CNT Film grown at 700 °C. (c) Fe catalyst on the top of the CNTs. (d-f) The top-view SEM images of the CNT bundle prepared from the CNT Film.**

The enlarged surface structure was shown in the high magnification TEM image. The tubular nanostructure was found in the image of Fig. 2, and the wall thickness was ~11 nm. Fe catalyst promoting the VLS growth was presented on the top of the CNTs, similar to the SEM image in Fig. 1(c).

The Raman characteristics of CNT film were examined in Fig. 3. The typical D band (caused by disordered structures of graphene) and G band (arising from the stretching of the C-C bond in graphitic materials) were located at 1356 cm-1 and 1593 cm-1, respectively. (George *et al*. 2005) The ID/IG ratio was 0.753, which was acquired in the peak intensity values. This value indicated high graphitic crystallization of CNT film.

In terms of exposure to $N_2$ gas filling and pumping environments, the change of electrical resistance of p-type CNT film was recorded in Fig. 4. (Varghese *et al*. 2001; Huang *et al*. 2005) The different biased voltages of 1V to 10V were applied on the CNT film at various $N_2$ gas concentrations from 0.05 Torr to 500 Torr. When the sample was exposed to a $N_2$ gas filling environment, the electrons transferred from absorbed $N_2$ gas to CNT film and then weakened the concentration of conducting holes in p-type CNT film, resulting in enlarged electrical resistance. (Huang *et al*. 2005; Zhao *et al*. 2002) In the case of the pumping environment, almost all the $N_2$ gas left the surface of CNT film so the electrical resistance returned back to its initial value. Therefore, the reversible interaction between $N_2$ gas and the surface of CNT film was considered as the physisorption behavior, caused by van der Waals forces. The $N_2$ gas absorption behavior was significantly enhanced through increasing the concentration of $N_2$ gas, which provided more opportunity to react with CNT film. Besides, higher biased voltages were found to promote the interaction between $N_2$ gas and the CNT film. The sensibility of CNT film was then enhanced as well.

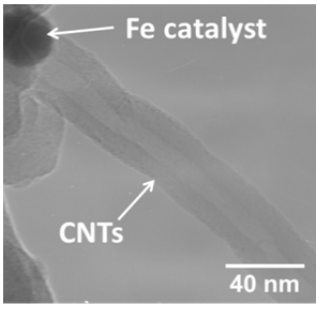


**Fig. 2 The TEM image of CVD-grown CNTs showing the tubular nanostructure.**

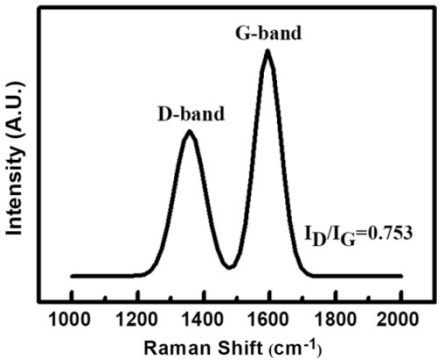


**Fig. 3 Raman spectrum for the CVD-deposited CNTs at 700 °C growth temperature.**

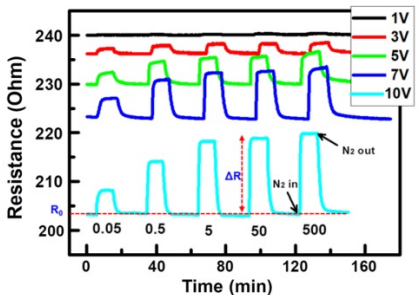


**Fig. 4 The electrical resistance of p-type CNT film was recorded in terms of the exposure to $N_2$ gas filling and pumping environments. The different biased voltages of 1V to 10V were applied on the CNT film at various $N_2$ gas concentrations from 0.05 Torr to 500 Torr.**

The sensitivity was defined as the ratio S = (ΔR/Ro) × 100%, where ΔR was the difference of the CNT resistance in the $N_2$-filling and pumping environment, and Ro represented the CNT resistance in a pumping environment. The sensitivity of two different concentrations of 0.5 Torr and 500 Torr for CNT film at various bias voltages was shown in Fig. 5. Upon exposure to a 0.5 Torr $N_2$ ambiance, the sensitivity of CNT film was improved from 0.05, 0.76, 2.05, 3.56 to 5.24 at an enlarged bias of 1V, 3V, 5V, 7V to 10V, respectively. Similarly, in the case of a 500 Torr $N_2$ environment, the sensitivity was enhanced more evidently from 0.08, 0.92, 2.86, 4.70 to 8.18. Both high $N_2$ gas concentrations and high voltages could promote $N_2$ gas absorption on the surface of CNTs, as it was mentioned before. The response time and recovery time were defined as the time when the change of resistance reached to 80% ΔR in the $N_2$-filling and pumping environment, respectively. The response time in a 500 Torr $N_2$ ambiance was 10 ~ 30 sec, but the response time in a 0.5 Torr $N_2$ ambiance was 40 ~ 50 sec, which was significantly slower. The CNT film in the 500 Torr $N_2$ ambiance had significantly faster response rate since a higher concentration of $N_2$ was provided, and the reaction sites on the CNTs were occupied quickly. However, the CNT film in the 0.5 Torr $N_2$ ambiance showed a faster recovery time of 120 ~ 150 sec, compared with the CNT film in the 500 Torr $N_2$ ambiance, which had the recovery time of 140 ~ 170 sec. The slower recovery rate for the CNT film in the 500 Torr $N_2$ ambiance might be resulted from the tardy return of electrons to the absorbed $N_2$ gas. The response time, recovery time, and the CNT film sensitivities in 0.5 Torr and 500 Torr at various voltage biases were listed in the table 1.

Figure 6 showed the electrical resistance and the sensitivities of the p-type CNT bundle in the $N_2$ gas filling and pumping environments. The electrical resistance of the CNT bundle, the nearly perfect electrical resistance, was recorded at two biased voltages of 5V and 10V in the different $N_2$ gas concentrations from 0.05 Torr to 500 Torr in Figs. 6(a) and (b). The physisorption behavior of $N_2$ gas on the surface of the CNT bundle rendered the electrical resistance reversible in each filling and pumping cycles. At the 5V bias, the sensitivities of the CNT bundle was increased from 1.1, 6.1, 12.1, 13.9, to 14.1, as the concentration of $N_2$ gas increased from 0.05, 0.5, 5, 50, to 500 Torr, respectively. Likewise, at the 10V bias, the sensitivity of the CNT bundle was significantly increased from 1.1, 7.8, 31.3, 40.8, to 42.6 as the concentration of $N_2$ gas increased from 0.05 to 500 Torr. Regardless of the differences in $N_2$ gas concentrations and voltages applied in the experiments, the sensibilities of CNT bundle was found to be increased significantly. This may be attributed to enlarged reaction opportunity and promoted interaction with each other. In the 5V and 10V biases, the response time of the CNT bundle in different $N_2$ gas concentrations was ~ 20 sec. However, the recovery time of CNT bundle was 30 ~ 60 sec at the 5V bias and 20~50 sec at the 10V bias. In other words, the CNT bundle in the 5V bias had slower recovery time than that in the 10V bias. It was suggested that a higher power bias provide more energy for absorbed $N_2$ gas to escape from the surface of the CNT bundle so that the recovery time would be shortened. The response time, recovery time, and the sensitivities of the CNT bundle at 5V and 10V biases in various $N_2$ gas concentrations were listed in the table 2.

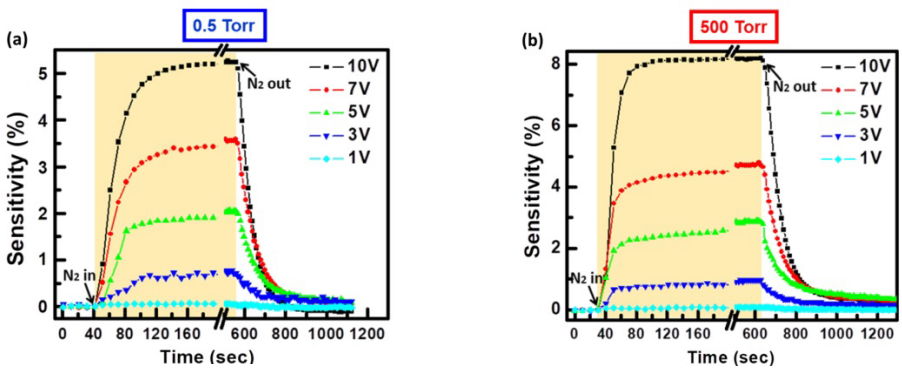


**Fig. 5 Exposed to (a) 0.5 Torr and (b) 500 Torr $N_2$ gas environments, the sensitivities of CNT film were measured at 1V to 10V biases.**

**Table 1 The response time, recovery time, and the sensitivities of the CNT film at various voltage biases were recorded in the environments of 0.5 Torr and 500 Torr $N_2$.**

| | Response time (sec) | | | | | Recovery time (sec) | | | | | Sensitivity (%) | | | | |
|---|---|---|---|---|---|---|---|---|---|---|---|---|---|---|---|
| | 1V | 3V | 5V | 7V | 10V | 1V | 3V | 5V | 7V | 10V | 1V | 3V | 5V | 7V | 10V |
| 0.5 Torr | 50 | 50 | 40 | 40 | 40 | 120 | 120 | 150 | 150 | 120 | 0.05 | 0.76 | 2.05 | 3.56 | 5.24 |
| 500 Torr | 10 | 20 | 20 | 20 | 30 | 170 | 160 | 160 | 160 | 140 | 0.08 | 0.92 | 2.86 | 4.70 | 8.18 |

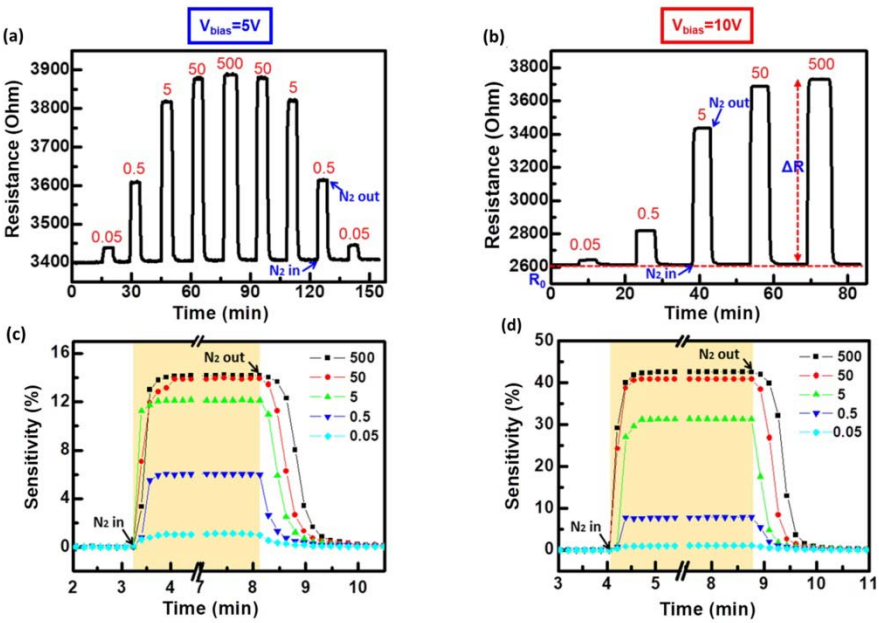


**Fig. 6 The electrical resistance and sensitivities of CNT bundle were recorded at 5V (a,c) and 10V (b,d) biases in the $N_2$ gas filling and pumping environments, respectively. The N2 gas concentrations were changed from 0.05 Torr to 500 Torr.**

**Table 2 The response time, recovery time, and the sensitivities of the CNT bundle at 5V and 10V biases in the various $N_2$ environments from 0.05 Torr to 500 Torr.**

| | response time (sec) | | | | | recovery time (sec) | | | | | sensitivity (%) | | | | |
|---|---|---|---|---|---|---|---|---|---|---|---|---|---|---|---|
| | 0.05 | 0.5 | 5 | 50 | 500 | 0.05 | 0.5 | 5 | 50 | 500 | 0.05 | 0.5 | 5 | 50 | 500 |
| 5V | 20 | 20 | 20 | 20 | 20 | 50 | 30 | 40 | 50 | 60 | 1.1 | 6.1 | 12.1 | 13.9 | 14.1 |
| 10V | 20 | 20 | 20 | 20 | 20 | 50 | 20 | 20 | 40 | 50 | 1.1 | 7.8 | 31.3 | 40.8 | 42.6 |

In order to investigate the effects of the geometric structures of CNT film and CNT bundle on $N_2$ detecting ability, the sensibilities of these two nanotubes were compared in Fig. 7. The CNT bundle showed significantly much higher sensitivities (12.1 and 31.3), comparing to the sensibility of the CNT film (2.2 and 7.4), at the 5V and 10V biases, respectively. The $N_2$ filling environment was 5 Torr. Dr. Zhao claimed that the location of absorbed gas on CNTs could be at interstitial, groove surface and pore sites. Adsorption energy Ea (meV) was 174, 114, 111, and 94, and the charge transfer Q was 0.035, 0.026, 0.012, and 0.014, respectively. (Zhao *et al*. 2002) These interstitial and groove sites not only had higher adsorption energy but also served as preferred anchorage to produce stronger charge transfer. Since CNT bundle was intensively and systematically arranged in order, it would provide abundant interstitial and groove absorptions sites, resulting in strong absorption and high sensitivity to $N_2$ gas. Besides, the CNT bundle demonstrated significantly faster responses time (20 sec) and recovery time (20 ~ 40 sec) than the CNT film (30 sec in response time, 120 ~ 150 sec in recovery time). These results might be ascribed to the quick absorption and escaping reaction of $N_2$ gas in and out of the interstitial and groove sites. The response time, recovery time, and the sensitivities of the CNT film and bundle at 5V and 10V biases in 5 Torr $N_2$ gas concentration were listed in the table 3.

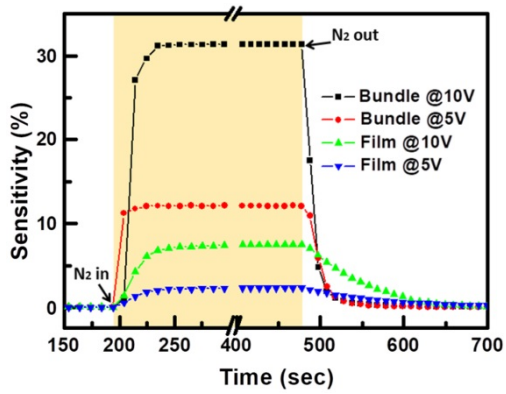


**Fig. 7 The sensitivities of CNT film and bundle were measured at 5V and 10V biases in the $N_2$ gas filling and pumping environments. The $N_2$ gas concentration was 5 Torr.**

**Table 3 The response time, recovery time, and sensitivities of the CNT film and bundle at 5V and 10V biases in the 5 Torr $N_2$ environment.**

| | response time (sec) | | recovery time (sec) | | sensitivity(%) | |
|---|---|---|---|---|---|---|
| | 5V | 10V | 5V | 10V | 5V | 10V |
| Bundle | 20 | 20 | 40 | 20 | 12.1 | 31.3 |
| Film | 30 | 30 | 150 | 120 | 2.2 | 7.4 |

## 4. CONCLUSION

In this study, the CVD-grown CNT film and bundle were investigated as $N_2$ gas detector. In the environment of 10V bias and 500 Torr $N_2$, the CNT bundle had fast response time (20 sec), recovery time (50), and excellent sensitity to $N_2$ gas (42.6), respectively. However, the CNT film was less responsive to $N_2$ gas, 30 sec in response time, 140 sec in recovery time, and 8.18 in $N_2$ sensitivity. It was believed that the unique geometric structure of the CNT bundle could provide abundant interstitial and groove sites for $N_2$ gas absorption and charge tranfer. This study confirmed that the geometric structures of CNTs would affect the detection of $N_2$ gas.

## ACKNOWLEDGMENTS

This research was supported by Ministry of Science and Technology (MOST105-2112-M-224-001) and National Yunlin University of Science and Technology (108T01 and 108T04).

## REFERENCES

Cantalini, C., Valentini, L., Lozzi, L., Armentano, I., Kenny, J.M., and Santucci, S. (2003). "$NO_2$ gas sensitivity of carbon nanotubes obtained by plasma enhanced chemical vapor deposition." *Sensors and Actuators. B, Chemical*, **93**, 333-337.

Chang, Y.-H., Lin, H.-W., and Chen, C. (2012). "Growth mechanism of self-assembled $TiO_2$ nanorod arrays on Si substrates fabricated by Ti anodization." *Journal of The Electrochemical Society*, **159**, D512-D517.

Chang, Y.-H., Lin, C.-T., Chen, T.-Y., Hsu, C.-L., Wei, K.-H., and Li, L.-J. (2013). "Highly Efficient Electrocatalytic Hydrogen Production by MoSx Grown on Graphene-Protected 3-Dimensional Ni Foam." *Advanced Materials*, **25**, 756-760.

Chang, Y.-H., Nikam, R.D, Lin, C.-T., Huang, J.-K., Tseng, C.-C., Hsu, C.-L., Cheng, C.-C., Su, C.-Y., Li, L.-J., and Chua, D. H.C. (2014). "Enhanced Electrocatalytic Activity of $MoS_x$ on TCNQ-treated Electrode for Hydrogen Evolution Reaction." *ACS Applied Materials & Interfaces*, **6**, 17679-17685.

Chang, Y.-H., Zhang, W., Zhu, Y., Han, Y., Pu, J., Chang, J.-K., Hsu, W.-T., Huang, J.-K., Hsu, C.-L., Chiu, M.-H., Takenobu, T., Li, H., Wu, C.-I, Chang, W.-H., Wee, A.T.S., and Li, L.-J. (2014). "Monolayer $MoSe_2$ Grown by Chemical Vapor deposition for Fast Photodetection." *ACS Nano*, **8**, 8582-8590.

Chang, Y.-H., Wu, F.-Y., Chen, T.-Y., Hsu, C.-L., Chen, C.-H., Wiryo, F., Wei, K.-H., Chiang, C.-Y., and Li, L.-J. (2014). "Three-Dimensional Molybdenum Sulfide Sponges for Electrocatalytic Water Splitting." *Small*, **10**, 895-900.

Chang, Y.-H., Chen, Y.-T., Huang, C.-S., Lu, C.-L., Lee, S.-H., Huang, B.-R., and Chen, C. (2018). "Growth Mechanism of Self-Assembled $Ti_xW_yO$ Nanotubes Fabricated by TiW Alloy Anodization." *Journal of The Electrochemical Society*, **165**, D1-D5.

Chopra, S., Phama, A., Gaillard, J., Parker, A., and Rao, A.M. (2002). "Carbon-nanotube-based resonant-circuit sensor for ammonia." *Applied Physics Letters*, **80**, 4632-634.

Chopra, S., McGuire, K., Gothard, N., and Rao, A.M. (2003). "Selective gas detection using a carbon nanotube sensor." *Applied Physics Letters*, **83**, 2280-2282.

Collins, P.G., Bradley, K., Ishigami, M., and Zettl, A. (2000). "Extreme Oxygen Sensitivity of Electronic Properties of Carbon Nanotubes." *Science*, **287**, 1801-1804.

Futaba, D.N., Hata, K., Yamada, T., Hiraoka, T., Hayamizu, Y., Kakudate, Y., Tanaike, O., Hatori, H., Yumura, M., Iijima, S. (2006). "Shape-engineerable and highly densely packed single-walled carbon nanotubes and their application as super-capacitor electrodes." *Nature Materials*, **5**, 987-994.

George, R., Kashyap, K., Rahul, R., and Yamdagni, S. (2005). "Strengthening in carbon nanotube/aluminium (CNT/Al) composites." *Scripta Materialia*, **53**, 1159-1163.

Huang, C.S., Huang, B.R., Jang, Y.H., Tsai, M.S., and Yeh, C.Y. (2005). Three-terminal CNTs gas sensor for $N_2$ detection." *Diamond & Related Materials*, **14**, 1872-1875.

Jang, Y.-T., Moon, S.-II, Ahn, J.-H., Lee, Y.-H., and Ju, B.-K. (2004). "A simple approach in fabricating chemical sensor using laterally grown multi-walled carbon nanotubes." *Sensors and Actuators. B, Chemical*, **99**, 118-122.

Kong, J., Franklin, N. R., Zhou, C., Chapline, M.G., Peng, S., Cho, K., and Dai, H. (2000). "Nanotube Molecular Wires as Chemical Sensors." *Science*, **287**, 622-625.

Korotcenkov, G. (2007). "Metal oxides for solid-state gas sensors: What determines our choice?" *Materials Science and Engineering: B*, **139**, 1-23.

Lee, W. and Park, S.-J. (2014). "Porous anodic aluminum oxide: anodization and templated synthesis of functional nanostructures." *American Chemical Society*, **114**, 7487-7556.

Liang, Y.X., Chen, Y.J., and Wang, T.H. (2004). "Low-resistance gas sensors fabricated from multiwalled carbon nanotubes coated with a thin tin oxide layer." *Applied Physics Letters*, **85**, 666-668.

Li, J., Lu, Y., Ye, Q., Cinke, M., Han, J., and Meyyappan, M. (2003). "Carbon Nanotube Sensors for Gas and Organic Vapor Detection." *Nano Letters*, **3**, 929-933.

Lin, H.-W., Chang, Y.-H., and Chen, C. (2012). "Facile Fabrication of $TiO_2$ Nanorod Arrays for Gas Sensing using Double-Layered Anodic Oxidation Method." *Journal of The Electrochemical Society*, **159**, K5-K9.

Modi, A., Koratkar, N., Lass, E., Wei, B., and Ajayan, P.M. (2003). "Miniaturized gas ionization sensors using carbon nanotubes." *Nature*, **424**, 171-174.

Novoselov, K.S., Geim, A.K., Morozov, S.V., Jiang, D., Zhang, Y., Dubonos, S.V., Grigorieva, I.V., and Firsov, A.A. (2004). "Electric Field Effect in Atomically Thin Carbon Films." *Science*, **306**, 666-669.

Qi, P., Vermesh, O., Grecu, M., Javey, A., Wang, Q., Dai, H., Peng, S., and Cho, K.J. (2003). "Toward large arrays of multiplex functionalized carbon nanotube sensors for highly sensitive and selective molecular detection." *Nano Letters*, **3**, 347-351.

Ong, K.G., Zeng. K., and Grimes, C.A. (2002). "A wireless, passive carbon nanotube-based gas sensor." *IEEE Sensors Journal*, **2**, 82-88.

Tang, H., Prasad, K., Sanjinés, R., and Lévy, F. (1995). "$TiO_2$ anatase thin films as gas sensors." *Sensors and Actuators. B, Chemical*, **26**, 71-75.

Tomchenko, A.A., Harmer, G.P., Marquis, B.T., and Allen, J.W. (2003). "Semiconducting metal oxide sensor array for the selective detection of combustion gases." *Sensors and Actuators B: Chemical*, **93**, 126-134.

Varghese, O.K., Kichambare, P.D., Gong, D., Ong, K.G., Dickey, E.C., and Grimes, C.A. (2001). "Gas sensing characteristics of multi-wall carbon nanotubes." *Sensors and Actuators. B, Chemical*, **81**, 32-41.

Villalpando-Pàez, F., Romero, A.H., Muñoz-Sandoval, E., Martínez,

L.M., Terrones, H., and Terrones, M. (2004). "Fabrication of vapor and gas sensors using films of aligned CNx nanotubes." *Chemical Physics Letters*, **386**, 137-143.

Wagner, R.S. and Ellis, W.C. (1964). "Vapor-liquid-solid mechanism of single crystal growth." *Applied Physics Letters*, **4**, 89-90.

Wong, Y.M., Kang, W.P., Davidson, J.L., Soh, A., and Wisitsora-at, K.L. (2003). "A novel microelectronic gas sensor utilizing carbon nanotubes for hydrogen gas detection." *Sensors and Actuators. B, Chemical*, **93**, 327-332.

Xia, Y., Yang, P., Sun, Y., Wu, Y., Mayers, B., Gates, B., Yin, Y., Kim, F., and Yan, H. (2003). "One-dimensional nanostructures: synthesis, characterization, and applications." *Advanced Materials*, **15**, 353-389.

Zhao, J., Buldum, A., Han, J., and Lu, J.P. (2002). "Gas molecule adsorption in carbon nanotubes and nanotube bundles." *Nanotechnology*, **13**, 195-200.